Flow pattern maps, pressure drop and performance assessment of horizontal tubes with coiled wire inserts during condensation of R-600a

Article (Accepted Version)

Flow pattern maps, pressure drop and performance assessment of horizontal tubes with coiled wire inserts during condensation of R-600a

Hadi Ahmadi Moghaddam[a,b], Alireza Sarmadian[c], Maziar Shafaee[a*], Hamid Enayatollahi[c]

[a]Faculty of New Sciences and Technologies, University of Tehran, Tehran, Iran.

[b]Center of Excellence in Design and Optimization of Energy Systems, College of Engineering, University of Tehran, Tehran, Iran

Email: ahmadi.hadi@ut.ac.ir

[c]Department of Engineering and Design, University of Sussex, Brighton BN1 9QT, UK.

Email: a.sarmadian@sussex.ac.uk , h.enayatollahi@sussex.ac.uk

*Corresponding author, Email: mshafaee@ut.ac.ir, Tel.: +98-919-0110200; fax: +98-21-88497324

Abstract

An experimental study is conducted to determine the pressure drop of refrigerant R-600a during forced convection condensation within a horizontal smooth pipe and spiral coil inserted pipes. Then, the system performance factor is calculated to evaluate the effectiveness of the inserts based on the pressure drop and heat transfer data. Test runs were done for varied vapor qualities between 0.05-0.79 and mass velocities between 115-365 $kgm^{-2}s^{-1}$. The test condenser was a pipe constructed from copper with the length and internal diameter of 1000 and 8.1 mm, respectively. Five coiled wires with varied wire thicknesses and coil pitches were utilized in the full length of the test section. Results revealed that the pressure drops in rough tubes were 1.51-11.97 times of those in the smooth tube. It was also observed that by decreasing the wire diameter and increasing the coil pitch, the pressure loss decreases. Results demonstrated that using inserts at higher mass fluxes results in higher performance factors. Based on the current empirical results, a new correlation is suggested for predicting the pressure drops of R-600a during condensation inside spiral coil inserted pipes. Furthermore, the flow pattern maps showed that inserting coiled wires postpones the transition from annular to intermittent.

Keywords: *Condensation; Coiled wire; Correlation; Flow pattern; Pressure drop; R-600a.*

Nomenclature

d	Tube diameter(mm)
e	Wire diameter (m)
Fr	Froude number
G	Mass velocity ($kgm^{-2}s^{-1}$)
LO	Liquid only
PDR	Pressure drop ratio
PF	Performance factor

p	Pressure (kPa)
P	Coil pitch (m)
Re	Reynolds number
VO	Vapor only
We	Weber number
x	Vapor quality

Greek symbols

θ	Helix angle of coiled wire (degree)
$\emptyset$	Chisholm correlation factor
α	Zivi void fraction
μ	Viscosity
ϕ	Two-phase multiplier
ρ	Density
σ	Surface tension

Subscripts

c	Coiled wire insert
ch	Chisholm
e	Equivalent
$fric$	Frictional
g	Vapor phase
in	Inlet
l	Liquid phase
mom	Momentum
r	Rough
s	Smooth
tc	Test condenser
tot	Total

1. Introduction

Within recent decades, so many efforts have been made to reduce the energy usage and improve the overall efficiency in different industrial systems such as heat exchangers. Employing inserts as turbulators inside heat exchangers is an example for these aims [1]. The inserts such as coiled wires are found to be efficacious in heat exchangers by enhancing the heat transfer rate significantly. Therefore, when using heat exchangers for different purposes such as conversion or recovery of energy in thermal processing of chemical, generation of steam, cogeneration plants, air-conditioning, sensible heating, recovery of waste heat, heating of fluids in manufacturing, and condensation process in power, it is possible to install the inserts inside the heat exchangers to promote the thermal performance [2, 3]. The drawback of this method, i.e. installing coiled wires, is that a considerable amount of pressure drop is always imposed to the system. Therefore, it is extremely important to take into account the impacts of coiled wires on both heat transfer

and pressure drop to make deductions about the usefulness of these instruments in refrigeration applications. Also, having the ability of pressure drop prediction plays a prominent role in the modified design of modern heat exchangers.

Employing coiled wires although improves the heat transfer coefficient in single-phase flow [4-6] and two-phase flow heat exchangers [7-9], as is reported by researchers previously, it is accompanied by a substantial pressure drop which has to be considered in designing such heat exchangers. In this regard, Akhavan-Behabadi et al. [10] experimentally investigated the pressure drop rise of refrigerant R-134a as a consequence of installing springs during condensation inside a horizontally placed pipe. Spiral coils with different geometrical features were tested under different vapor qualities and mass fluxes. Observations illuminated that the pressure loss in coiled wire inserted tubes (rough tubes) is 2.6-16 times of that in the smooth tube. In this study, a correlation was also developed to predict the pressure loss of R-134a in rough pipes. Within another empirical study, Akhavan-Behabadi et al. [11] evaluated the evaporation of refrigerant R-134a inside horizontal pipes with springs. It was concluded that springs contribute to the heat transfer augmentation, but a pressure drop increase of 1000% over the smooth tube was also experienced. However, these studies were conducted on evaporation or condensation of R-134a which has a high global warming potential (GWP) and the use of this refrigerant is not recommended anymore considering the global warming concerns. Jalil and Goudarzi [12] empirically assessed the performance of an evaporator when different mass flow rates between 0.167-0.583 kgs^{-1} were applied to the system and various instruments such as coiled wires, modified coiled wires, and butterfly inserts were utilized. Regarding the coiled wires, the experimental data suggested that employing these inserts with coil pitch to wire diameter ratios (p/e) of 20 and 10 is helpful as the system overall performance was improved. However, by increasing this ratio beyond 20, the performance factor was below one.

Regarding the single phase flows, Sharafeldeen et al. [13] performed an experiment to reveal the impacts of springs on heat transfer and pressure loss of air, when the Reynolds number was variable and the heat flux was applied to the system uniformly. Generally, the tests demonstrated a sizeable growth in both transferred heat and friction factor over the plain pipe. The results indicated that by using wire coils with larger wire diameters and smaller pitches, higher pressure drops for air are obtained. Finally, new correlations for the prediction of Nusselt number and friction factor were proposed. The deviation of pressure loss amounts obtained by the correlation from the empirical data was within the range of ±6%. Du et al. [14] evaluated the influence of wire coils with different arrangements when air was flowing inside rough test pipes. Again, increases in both friction factor and heat transfer were observed. According to the reports, the friction factor in rough pipes was 1.74-2.26 times of that in smooth pipes. Recently, Abdul Hamid et al. [15] evaluated the thermal performance of a heat exchanger by considering various operating conditions and employing various spiral coils and TiO_2-SiO_2 nano-fluids so as to augment the system heat transfer. According to the observations, the inserts gave rise to the frictional pressure drop and heat transfer rate. Considering the performance factor which was above one using inserts for all nano-fluids concentrations, it was suggested the utilization of spiral coils is beneficial.

One important consideration in different industrial applications is using environment-friendly refrigerants. Recently, the use of environment-friendly refrigerants has received more attention due to the growing concerns of environmental issues [16]. In this regard, some restricting rules are established to forbid or limit the use of traditional refrigerants. For instance, using refrigerant R-12 has been stopped because of its ozone depleting potential (ODP). Also, R-134a usage must be reduced because this refrigerant has high global warming potential, although it has appropriate thermodynamic properties [17, 18].

Due to the importance of using environment-friendly refrigerants and appropriate features of R-600a as a natural refrigerant, many investigations have been focused on the performance of this fluid in refrigeration systems within recent years. In this regard, an empirical investigation was carried out by Copetti et al. [19] to appraise the heat transfer and pressure loss of R-600a during evaporation inside a horizontal pipe with the internal diameter of 2.6 mm. The experimental results illuminated that frictional pressure loss grows as the vapor qualities and mass fluxes increase. It was also found that compared to R-134a, the obtained heat transfer rate and pressure losses by R-600a were larger. Another investigation conducted experimentally by Wen et al. [20] on evaporation of R-600a within rough tubes demonstrated that by increasing the mass flux, higher heat transfer rates are achievable. Meanwhile, the inserts augmented both heat transfer and pressure drop. Oliveira et al. [21] made a comparison between the pressure loss of R-600a and R-290 during evaporation inside horizontally installed pipes for mass fluxes between 240-480 $kgm^{-2}s^{-1}$. It was illustrated by the experiments that the pressure loss obtained during the evaporation of R-600a is larger than that of R-290. In another research performed by Yang et al. [22] on evaporation of R-600a and R-1234ze(E) in horizontal pipes under different saturation pressures and mass and heat fluxes, it was demonstrated that using R-600a results in higher heat transfer coefficients and pressure losses as compared to R-1234ze(E). Recently, Moghaddam et al. [23] investigated the heat transfer performance of R-600a during condensing inside horizontal smooth and spiral coil inserted pipes. For this purpose, vapor qualities between 0.03-0.79 and mass fluxes within the range of 115-365 $kgm^{-2}s^{-1}$ were considered during tests. Also, spiral coils with different coil pitches and wire diameters were installed inside the test pipe. The experiments revealed that by increasing the vapor quality and mass velocity, the heat transfer coefficients enhance. Also, it was observed that inserting wire coils enhances the heat transfer rate and influences the transitions of the flow patterns.

In this research, considering the necessity of further evaluating and introducing environment-friendly refrigerants, the natural refrigerant R-600a is used and its pressure drop characteristics during forced convective condensation within horizontal plain and wire coil inserted pipes are assessed. The ODP of this refrigerant is zero. Also, the GWP of this refrigerant is insignificant [24]. Furthermore, R-600a has other good thermodynamic properties which make it an appropriate candidate for use in refrigeration applications. For instance, R-600a owns higher liquid thermal conductivity compared to R-134a, which would contribute to the better heat transfer. Also, the liquid viscosity of R-600a is comparatively low which would result in higher liquidity in heat exchangers [25]. The open literature survey shows that the condensation pressure loss of R-600a inside horizontal coiled wire inserted pipes has not been studied previously. In the second part of this work, the effectiveness of the inserts is evaluated by

calculating the performance factor. For this purpose, the current pressure drop data and previous heat transfer results [23] are used. Furthermore, a new correlation is developed for prediction purposes by employing an empirical model which is of paramount importance to further design efforts. Finally, new flow pattern maps are presented for condensation of R-600a within horizontal smooth and coiled wire inserted tubes.

2. Experimental test facilities design

The present refrigeration cycle is consisted of test condenser, post condenser, flow meters, gear pumps, heaters, reservoir, pressure indicators, thermocouples, sight glasses, and differential pressure drop transducers. There are two loops constituting the cycle. The first loop is charged with R-600a and the second loop is charged with water for eliminating the refrigerant latent heat. The cooling water temperature was between 14-16 ^{o}C. Fig. 1 demonstrates the overall schematic view of the empirical test setup.

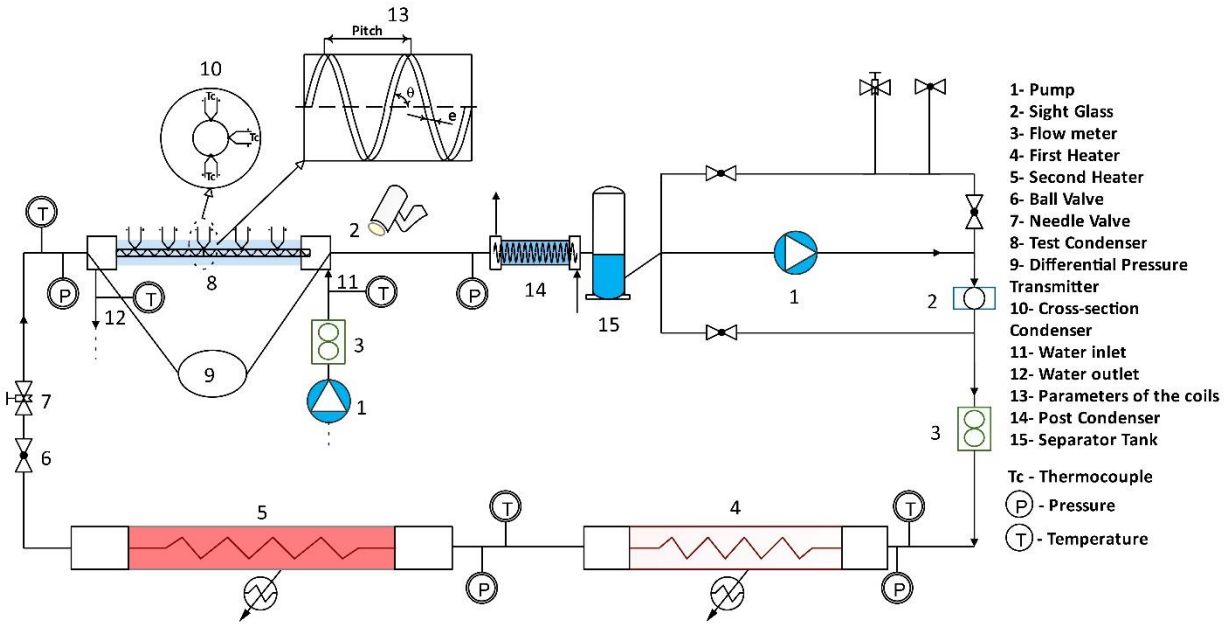

Fig. 1. Schematic configuration of the refrigeration cycle tested in this research.

Prior to performing the tests and to ensure that there is no leakage of gas from the cycle, firstly the cycle was filled with dry (oxygen free) nitrogen until it could reach the main experiment pressure of about 5 bar. The pressure gauges were also attached to the cycle. The system were kept under this condition for one day and the data were collected regularly to make sure there is no gas leakage.

In order to circulate and control the mass velocities of refrigerant R-600a and cooling water, two gear pumps with variable frequency and the power of 0.5 HP were utilized. In each loop, a flow meter having the precision of 0.1% of the full scale was placed after the pump for measuring the mass flow rates. To reach the desired vapor quality prior to entering the test condenser, two electrical resistance heaters with the power of 6 kW were used. Insulators were utilized around

these heaters to minimize the heat loss to the environment. A watt transducer was used to measure the supplied power by the heaters. The refrigerant enthalpy at the inlet of the heaters was obtained by using a platinum 100 RTD type sensor and a pressure transducer. The investigated condenser was a counter-flow coaxial double-pipe heat exchanger. The condenser inner pipe was made up of copper and its length, internal diameter, and thickness were 1000, 8.1, and 0.71 mm, respectively. The R-600a passes through the internal pipe and the water moves in a counter-flow direction through the annulus.

Two kinds of horizontal pipes including smooth pipe and spiral coil inserted pipes were employed to perform tests. Table 1 presents the geometrical features of the test tubes.

Table 1. Geometrical characteristics of the used coiled wire inserts.

Tube set	P (mm)	e (mm)	θ (degree)	Tube internal diameter (d_{in}) (mm)	d_e (mm)
Smooth	-	-	-	8.1	8.1
CW1	10	0.5	67.27	8.1	6.92
CW2	30	1	36.63	8.1	6.89
CW3	20	1	48.12	8.1	6.68
CW4	10	1	65.85	8.1	5.99
CW5	10	1.5	64.25	8.1	5.23

T-type thermocouples were used at five axial locations with a distance of 200 mm from each other for measuring the wall outside temperature of the inner tube. For this purpose, at each axial position, three thermocouples were attached to the top, bottom, and side of the test tube by welding. The precision of the sensors was 0.1 ℃. The sensors were connected to a 24-channel data logger (Lutron-4208 SD) to register the measurements, and the data logger was connected to a computer. Also, two calibrated RTD PT 100 temperature sensors were attached to the shell boundaries to capture the water temperatures. To measure the inlet pressure of the examined section, a pressure gauge (EN 837-1 Wika model) with the precision of 1 kPa was used. Also, to measure the pressure drop along the test section, a pressure transducer sensor (PDM-75) with the accuracy of 0.075% of the full scale was utilized in the cycle. This sensor was capable of measuring the pressure drops between 0-150 kPa. The employed refrigerant in the cycle was R-600a with the purity of 99.55%. A post condenser and a reservoir were utilized between the test condenser and the pump for making sure that the refrigerant is completely sub-cooled before flowing inside the pump. A sight glass is used just after the test condenser to observe the flow patterns. The sight glass, made from Pyrex glass, had the internal diameter and length of 8.1 and 200 mm, respectively. A digital camera was also used to capture the flow patterns. The range of operational conditions of the present empirical study are shown in Table 2.

Table 2. Operational parameters of the current research.

Parameter	Type or value	Units
Refrigerant	R-600a (Isobutane)	None
Cooling water temperature	14.1-16.3	℃
Refrigerant mass velocity	67-154	$kgm^{-2}s^{-1}$

Saturation temperature	38.5	℃
Average pressure	5.1	bar
Vapor quality	0.05-0.79	None

3. Data reduction

In the current empirical study, pressure losses of R-600a in the smooth and rough pipes, which were installed horizontally, are evaluated under various mass velocities of 67, 81, 98, 115, and 154 $kgm^{-2}s^{-1}$, and vapor qualities between 0.05-0.79. The data for any new state were collected 15 minutes after changing the system initial conditions to make sure that the system reaches the steady state conditions. 25% of the test runs for the case of smooth tube were conducted twice for checking the repeatability of the test facility.

Energy balance was carried out along the test condenser to determine the vapor quality at the test condenser boundaries (the inlet and outlet of the test section). Then, the mean of vapor qualities at the test section boundaries was assumed as the vapor quality of the whole test condenser, because the variations of the vapor quality along the test section was not significant. The method of calculating the vapor quality in details can be found in the previous research on heat transfer [23].

The total pressure drop is composed of momentum, static and frictional pressure drops:

$$\Delta P_{tot} = \Delta P_{mom} + \Delta P_{stat} + \Delta P_{fric} \quad (1)$$

As the studied tube was horizontal, the static pressure drop term is equal to zero. Therefore:

$$\Delta P_{tot} = \Delta P_{mom} + \Delta P_{fric} \quad (2)$$

To calculate the momentum pressure loss, Eq. (3) proposed by Collier and Thome [26] is used:

$$\Delta P_{mom} = G_{tot}^2 \left\{ \left[\frac{(1-x)^2}{\rho_l (1-\varepsilon)} + \frac{x^2}{\rho_g \varepsilon} \right]_{out} - \left[\frac{(1-x)^2}{\rho_l (1-\varepsilon)} + \frac{x^2}{\rho_g \varepsilon} \right]_{in} \right\} \quad (3)$$

Where $x, \rho, G,$ and ε represent vapor quality, density, mass velocity, and void fraction, respectively.

The void fraction for this flow regime is calculated by the correlation presented by Zivi [27]:

$$\alpha = \frac{1}{1 + (\frac{1-x_{tc}}{x_{tc}})(\frac{\rho_g}{\rho_l})^{2/3}} \quad (4)$$

To calculate the uncertainty in determining pressure losses during the experiments, a method proposed by Schultz and Cole [28] was used. Table 3 provides the test parameters and their uncertainties.

Table 3. Uncertainties of the measured quantities in this experiment.

Parameter	Uncertainty	Units
Thermocouples	0.1%	℃
Pressure drop transducer	0.075% of reading	Pa
Power	1% of reading	kWm^{-2}
Pressure sensors	1	kPa
Refrigerant mass flow rate	0.1% of reading	kgs^{-1}
Refrigerant mass velocity	17%	$kgm^{-2}s^{-1}$
Diameter	0.05	mm
Length	0.5	mm
Frictional pressure drop	7%	Pa
Vapor quality	6%	-

4. Results and discussion

In the following subsections, firstly, pressure losses of smooth pipe are measured and compared to those obtained by different correlations. Then, the pressure drop results are obtained for spiral coil inserted pipes and discussed. Furthermore, using the current pressure drop and previous heat transfer data [23], the system performance factor is assessed. In the next step, a correlation is developed based on the present empirical results to predict the pressure losses in spring inserted pipes. Finally, new flow pattern maps are provided for condensation of R-600a in smooth and rough pipes.

4.1. Pressure drops of the smooth tube

The trend of pressure drops changes with vapor quality for various mass velocities is illustrated in Fig. 2. As it is observable, the pressure drops rise when the vapor quality and the mass velocity augment. The reason behind this trend is that as the vapor quality grows, the velocity difference between the liquid and vapor phase increases which leads to a higher shear stress. Indeed, as it was discussed in previous studies [29, 30], the volume of vapor refrigerant augments by increasing the vapor quality resulting in the vapor velocity larger than that of the liquid refrigerant film. Consequently, the larger velocity difference between two phases results in higher shear stress and therefore higher pressure losses. Furthermore, the shear stress between the flow and the tube inner surface and coiled wire surface increases by increase of the mass velocity which gives rise to the pressure losses. Also, another ground for increase of the pressure loss with rise of the mass velocity is related to the growth in production of entrainments in the vapor refrigerant core and therefore rise in the redeposition of the produced entrainments to the liquid refrigerant film [29]. This phenomenon gives rise to the turbulent intensity in both the vapor core and the liquid film which results in higher shear stress. The more the shear stress, the more the pressure loss.

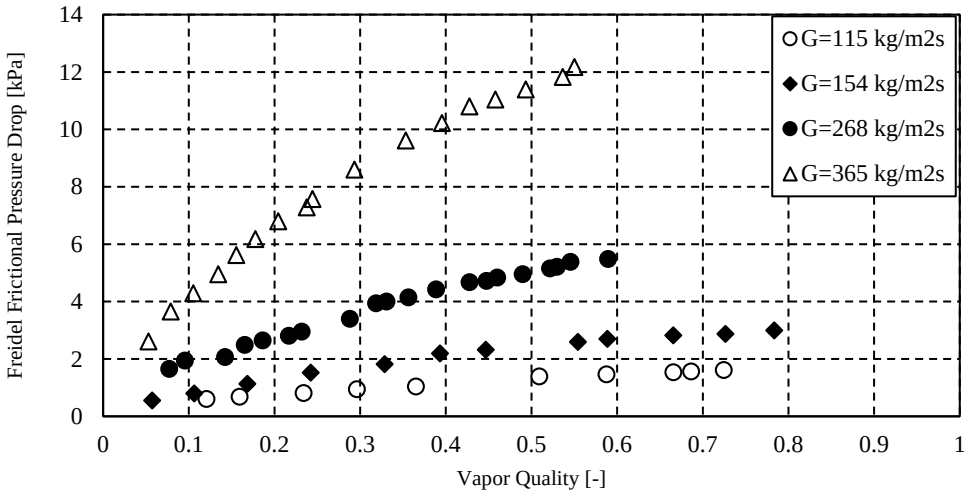

Fig. 2. The trend of frictional pressure drops changes with change of vapor quality for smooth tube.

The obtained pressure losses for the smooth pipe are compared to those obtained by available correlations to validate the results. For this purpose, proposed correlations by Chisholm [31], Müller-Steinhagen and Heck [32], and Friedel [33] are utilized. According to Fig. 3, the correlation proposed by Chisholm [31] shows a better agreement with the current empirical data. The average absolute deviation and the average deviation of the present empirical data from the Chisholm's correlation are 17.86 and 17.50%, respectively. It should be noticed that the semi-empirical correlations have been developed based on the limited data bases with specific experimental conditions. Therefore, it is possible that they fail to predict the empirical data properly. As it was concluded by Macdonald and Garimella [34], no correlation might be able to predict the empirical results accurately. Macdonald and Garimella [34] studied the condensation of propane under various conditions and then compared the obtained data with various correlations. They observed that there is no correlation capable of predicting the experimental data accurately. Similar observations were also reported by Ong and Thome [35] who examined thirteen various correlations using a vast range of data. They reported that there is no correlation capable of predicting the data in the error range of ±30%. Other research works also suggest similar observations. Dalkilic [36] evaluated various correlations against data obtained by R410a, R502, and R507a during condensation in horizontal pipes. It was reported that the best performing correlation was able to predict the experimental results within the range of ±30%. Accordingly, Song et al. [37] appraised twenty nine pressure drop correlations and reported that the best performing relation was able to predict the results within error band of ±30%. Similar conclusions were also drawn in other studies [38-41]. Indeed, based on the above-mentioned investigations, having the ability to predict the data in the error range of ±30% seems to be satisfactory in two-phase flow regimes. Based on the previous [9, 11] and current observations, it could be concluded that forced convective condensation or evaporation is severely an unstable and fully-turbulent phenomenon since the vapor phase and liquid phase flow together which is accompanied by transformation of phases.

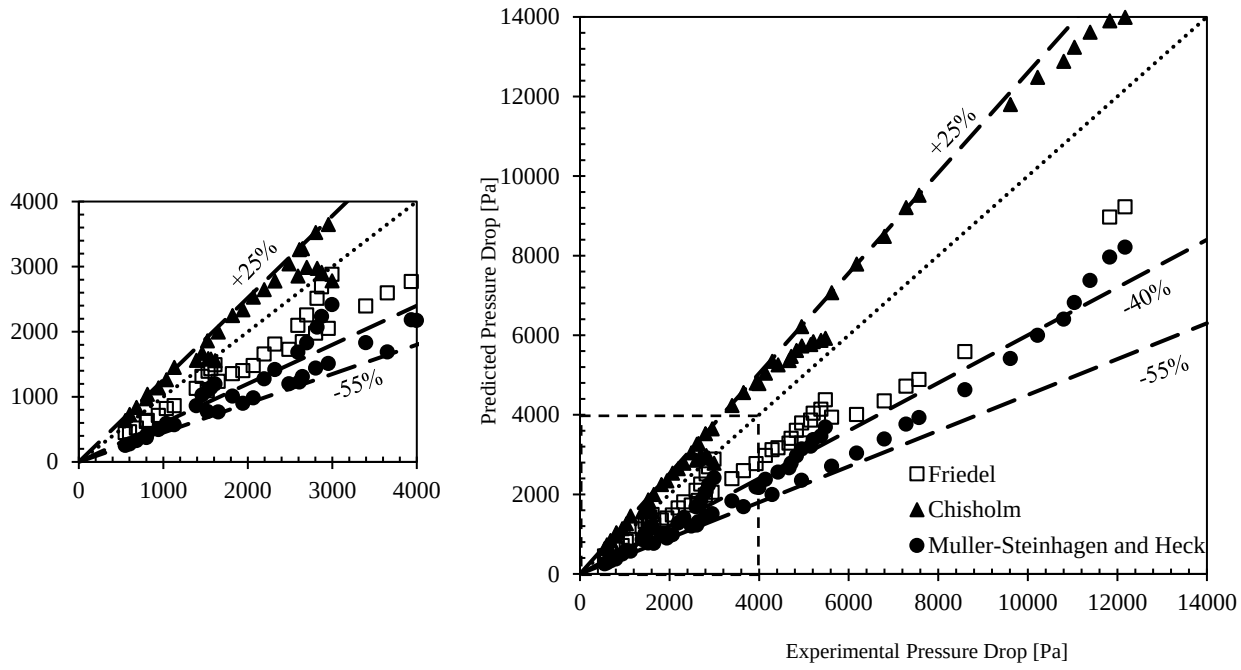

Fig. 3. Comparison between the frictional pressure drops obtained by current experiments and correlations.

The proposed correlation by Chisholm [31] for predicting the frictional pressure loss is:

$$\left(\frac{dp}{dz}\right)_{fric} = \left(\frac{dp}{dz}\right)_{l} \emptyset_{Ch}^{2} \tag{5}$$

Where $\emptyset_{Ch}^{2}$ representing Chisholm two-phase flow correlation factor is as follows:

$$\emptyset_{Ch}^{2} = 1 + (Y^{2} - 1)[Bx^{(2-n)/2}(1-x)^{(2-n)/2} + x^{2-n}] \tag{6}$$

Where B= 4.8, n= 0.25, and Y can be determined based on the gradient of liquid and gas frictional pressure loss:

$$Y^{2} = \frac{(dp/dz)_{g}}{(dp/dz)_{l}} \tag{7}$$

Where:

$$(\frac{dp}{dz})_l = f_l \frac{2G_{tot}^2}{d_i \rho_l} \quad (8)$$

275

276 And,

$$(\frac{dp}{dz})_g = f_g \frac{2G_{tot}^2}{d_i \rho_g} \quad (9)$$

277

278 Where f_L and f_G are friction factors for the single-phase state and expressed as:

$$f_l = \frac{0.079}{Re_l^{0.25}}, f_g = \frac{0.079}{Re_g^{0.25}} \quad (10)$$

279 And,

$$Re_l = \frac{G_{tot} d_i}{\mu_l}, Re_g = \frac{G_{tot} d_i}{\mu_g} \quad (11)$$

280 The correlation suggested by Müller-Steinhagen and Heck [32] is defined as follows:

$$(\frac{dP}{dL})_{tp-fr} = \left\{(\frac{dP}{dL})_{LO} + 2\left[(\frac{dP}{dL})_{VO} - (\frac{dP}{dL})_{LO}\right]x\right\}(1-x)^{0.33} + (\frac{dP}{dL})_{VO} x^3 \quad (12)$$

281 The single-phase all-liquid and vapor pressure gradients have been computed based on the all-
282 liquid and vapor Reynolds numbers. The single-phase friction factors for turbulent and laminar
283 flow regimes are as follows:

$$f = {}^{16}/_{Re}, \text{ for } Re < 1187 \quad (13)$$

$$f = 0.0791 Re^{-0.25}, \text{ for } Re > 1187 \quad (14)$$

284 The two-phase multiplier from Friedel [33] is as follows:

$$\Phi_{LO}^2 = A_1 + \frac{3.24 A_2 A_3}{Fr^{0.045} We^{0.035}} \quad (15)$$

285 Where We and Fr represent the Weber and Froude numbers, respectively. Furthermore, A_1, A_2,
286 and A_3 are dimensionless parameters as follows:

$$A_1 = (1-x)^2 + x^2 (\frac{\rho_L}{\rho_V})(\frac{f_{VO}}{f_{LO}}) \quad (16)$$

$$A_2 = x^{0.78} + (1-x)^{0.224} \quad (17)$$

$$A_3 = \left(\frac{\rho_L}{\rho_V}\right)^{0.91} \left(\frac{\mu_V}{\mu_L}\right)^{0.19} (1 - \frac{\mu_V}{\mu_L}) \quad (18)$$

4.2. Pressure drop of the coiled wire inserted tubes

Figs. 4-8 indicate the trend of pressure losses changes with variations of vapor quality under various mass velocities for coiled wire inserted tubes. It can be interpreted from the data that for any given mass velocity, the pressure drop increases by insertion of springs regardless of the inserts types. For instance, consider Fig. 4 showing the data related to tube set "CW1" with the smallest coil pitch and wire diameter. It can be seen that for all mass velocities, the insert "CW1" has led to rise in the pressure losses. Similarly, for other tube sets such as "CW2' with the largest coil pitch as shown in Fig. 5 or tube set "CW5" with the thickest wire diameter as shown in Fig. 8, similar trends have been observed. However, the magnitude of the pressure drop growth is dependent on vapor quality, mass velocity, and inserts types. Generally, it has been observed that at lower vapor qualities, the impacts of changes of vapor quality on the pressure drop is much significant compared to the high vapor qualities. In high vapor quality areas, i.e. vapor qualities higher than 0.6, it can be seen that the pressure drop changes slightly by increasing the vapor quality, but it changes sharply in low vapor quality areas. Further discussions about the impacts of different parameters such as mass flux and inserts are provided in the following.

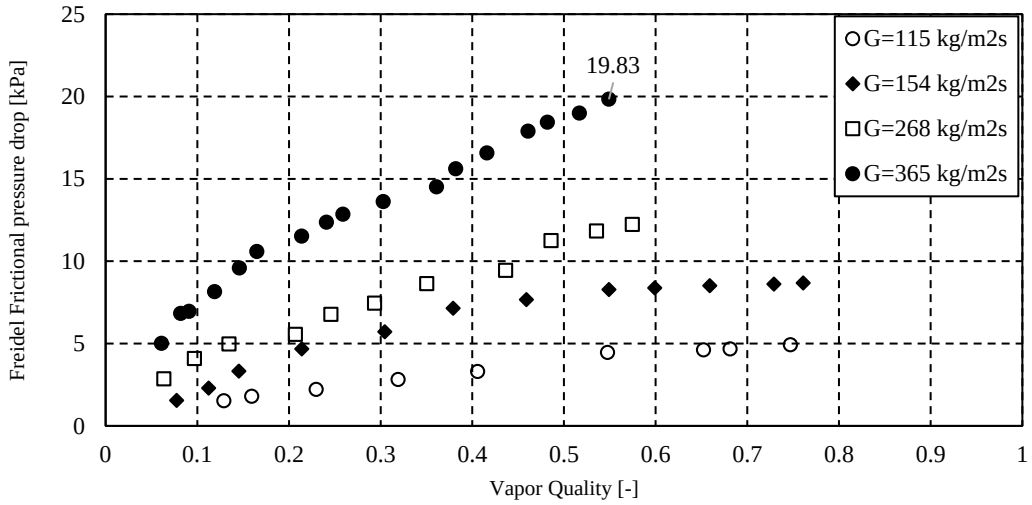

Fig. 4. The trend of frictional pressure drops changes with change of vapor quality for tube set 'CW1'.

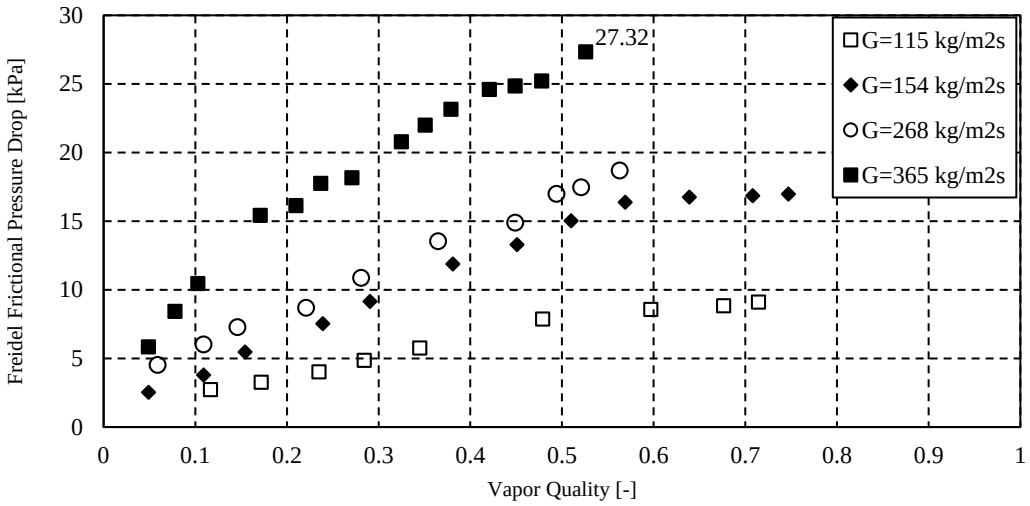

307

308 **Fig. 5.** The trend of frictional pressure drops changes with change of vapor quality for tube set 'CW2'.

309

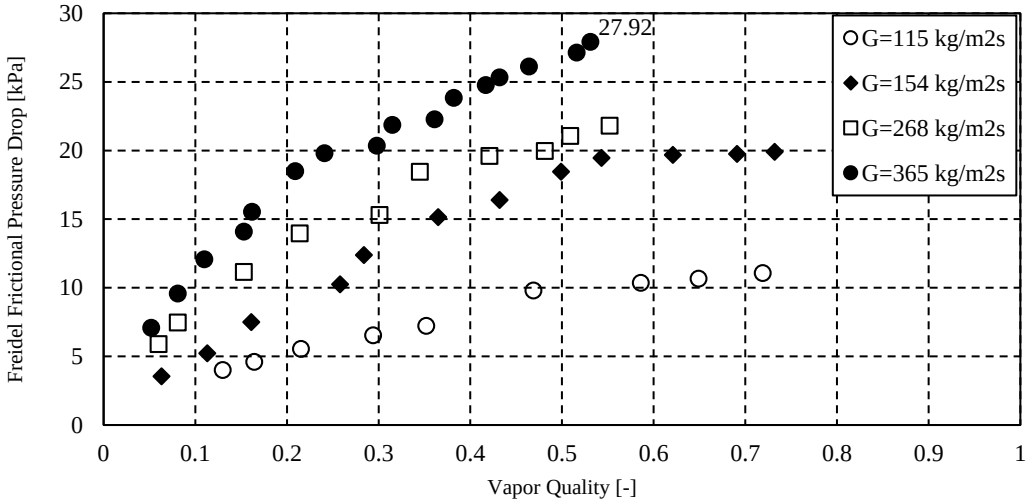

310

311 **Fig. 6.** The trend of frictional pressure drops changes with change of vapor quality for tube set 'CW3'.

312

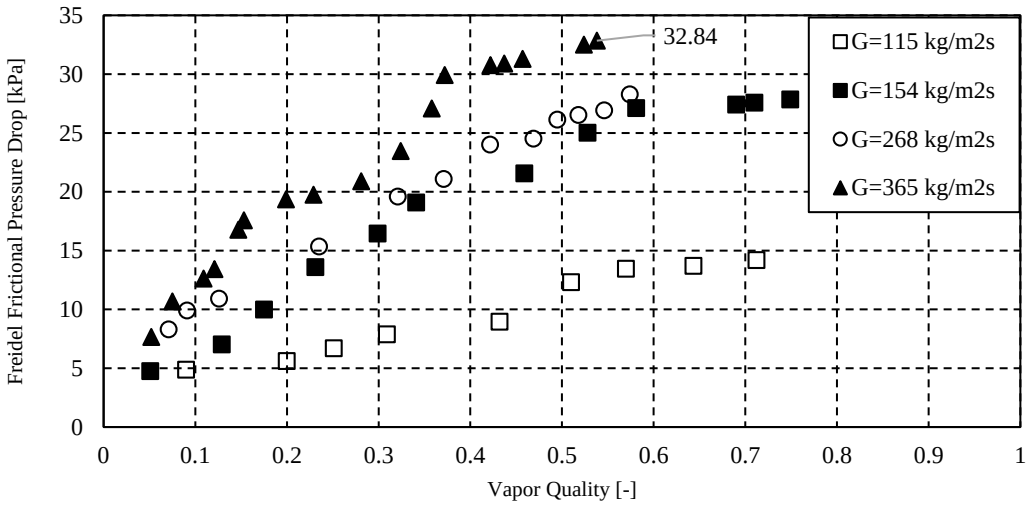

Fig. 7. The trend of frictional pressure drops changes with change of vapor quality for tube set 'CW4'.

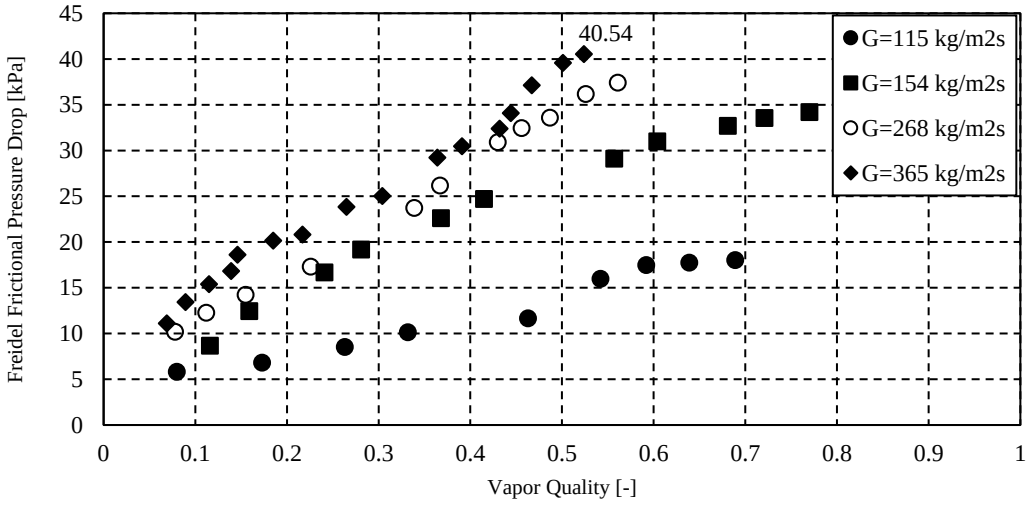

Fig. 8. The trend of frictional pressure drops changes with change of vapor quality for tube set 'CW5'.

To further investigate the role of inserts, Figs. 5-7 can be assessed in which the wire diameter is 1 mm and the coil pitch alters, i.e. 10 mm (CW4), 20 mm (CW3), and 30 mm (CW2). These plots illustrate that lowering the coil pitch leads to the pressure loss increment. Indeed, as the frictional surface per length of the pipe increases by the decrease of the coil pitch, the pressure loss escalates. For instance, for the mass velocity of 365 $kgm^{-2}s^{-1}$ and vapor qualities between 0.5-0.6, the highest pressure drops of 32.84, 27.92, and 27.32 kPa are obtained by using the tube

sets “CW4”, “CW3”, and “CW2”, respectively. This behavior is observed for any given vapor quality and mass velocity. Therefore, increasing the coil pitch will result in lower pressure drops.

Figs. 4,7,8 are illuminating the effects of coiled wires diameter when the coil pitch is 10 mm and the wire owns different diameters of 0.5 mm (CW1), 1 mm (CW4), and 1.5 mm (CW5). From these figures, it can be seen that thicker wires result in higher pressure drops. For instance, for the mass velocity of 365 $kgm^{-2}s^{-1}$ and vapor qualities between 0.5-0.6, the largest pressure losses of 40.54, 32.84, and 19.83 kPa are obtained by using the tube sets “CW5”, “CW4”, and “CW1”, respectively. Actually, as the wire diameter increases, the frictional surface increases too. Consequently, the frictional pressure loss grows. Furthermore, as it was discussed by Salimpour and Gholami [42], using thicker coiled wires results in a higher turbulence in the gas and liquid phases which causes the further increment of the frictional pressure loss. In addition, by utilizing thicker inserts flow cross-section area decreases, and accordingly the flow velocity increases which induces higher momentum pressure losses. Therefore, decreasing the wire diameter will lead to lower pressure losses.

The pressure drop ratio of the rough tubes to the smooth tube (PDR) for different mass fluxes is shown in Fig. 9. According to this plot, the ratio is much larger for lower mass fluxes. In higher mass fluxes, the effects of inserts fade because under these conditions (higher mass fluxes) the effects of flow velocity and momentum pressure loss are large enough. So, the impacts of inserts for higher mass velocities on pressure loss increment is not considerable as it is for lower mass velocities. For example, considering the tube set “CW5” it is observed that for the mass flux of 115 $kgm^{-2}s^{-1}$, the highest pressure drop ratio is 1197.36% meaning the pressure drop of the tube set “CW5” is almost 11.97 times of that for the smooth tube; while for the mass velocity of 365 $kgm^{-2}s^{-1}$, this value becomes 3.35.

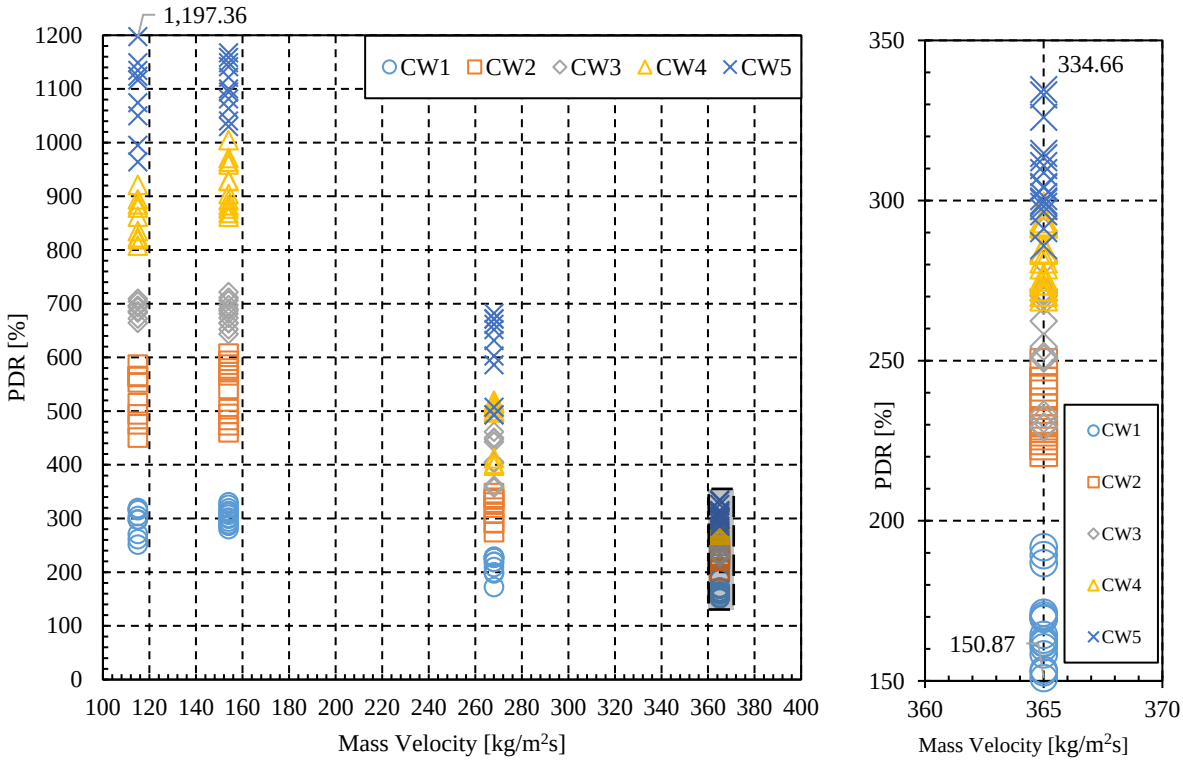

Fig. 9. Pressure drop ratio of the rough tubes to the smooth tube for different inserts and mass velocities (enlarged for the mass velocity of 365 kg/m^{2}s).

4.3. The system performance factor (PF)

The previously conducted research on the impacts of spiral coils on the heat transfer rate during condensation of R-600a in horizontal pipes demonstrated that the inserts contribute to the heat transfer enhancement [23]. On the other hand, the current data illuminated that these inserts also give rise to the pressure drop. Hence, to come to a conclusion regarding the effectiveness of the inserts, the performance factor is calculated and used as a criterion. For this purpose, the introduced parameter by Agrawal and Varma [43] as the ratio of the pumping power to the enhanced heat transfer coefficient is employed so as to evaluate the performance of the refrigeration system. The coiled wires result in pressure drop increments which in turn increase the pumping power. The following relation is used to calculate the pumping power [44, 45]:

$$W = \dot{v}\Delta P \tag{19}$$

In Eq. (19), $\dot{v}$ and ΔP are the volumetric flow rate and the pressure loss within the test pipe, respectively.

Then, the ratio of the pump consumed power to the smooth tube heat transfer coefficient, $(W/h)_s$, is calculated. Then, the same ratio is computed for the rough tubes. Finally, the ratio of $(W/h)_s$ to $(W/h)_r$ is determined as the performance factor.

$$PF = \frac{(W/h)_s}{(W/h)_r} = \frac{h_r/h_s}{(\Delta P)_r/(\Delta P)_s} = R_h/R_{\Delta P} \quad (20)$$

Where R_h shows the ratio of rough tube heat transfer coefficient to the smooth tube heat transfer coefficient. Also, $R_{\Delta P}$ demonstrates the ratio of rough tube pressure drop to the smooth tube pressure drop. If the performance factor is higher than one, it can be concluded that the coiled wires are advantageous. Otherwise, using these devices is not efficacious. The amounts of performance factor obtained by various inserts for different vapor qualities and mass velocities are demonstrated in Figs. 10 and 11.

It is observed that for all operating conditions of the system and inserts, the performance factor is below one suggesting that using coiled wires in condensation process within horizontal pipes is not recommended. Similar results were reported by Akhavan-Behabadi et al. [10] who evaluated the performance of a refrigeration cycle during condensation of R-134a inside horizontal tubes with coiled wires. Actually, the growth of pressure loss is too large, hence it can negate the positive impacts of heat transfer increase. Based on the obtained values, using these instruments is not satisfactory unless for specific cases where a compact heat exchanger is required or it is possible to justify the increased pumping power. The maximum and minimum obtained values of the performance factor are 0.93 (obtained by the largest mass flux) and 0.13 (obtained by the smallest mass flux), respectively. Indeed, at higher mass fluxes the growth of pressure drop is not as significant as in the small mass fluxes; but, the heat transfer coefficient growth is still considerable as shown previously in the related study [23]. According to Fig. 10, the highest performance factor is obtained by using “CW1” with the wire diameter of 0.5 mm and coil pitch of 10 mm.

To illuminate also the effects of vapor quality, Fig. 11 can be studied. This figure shows the highest values of the performance factors obtained in the highest and lowest mass fluxes for high vapor quality and low vapor quality areas. For the lowest mass velocity of 115 $kgm^{-2}s^{-1}$, the value of performance factor increases with the decrease of vapor quality for all the inserts, and they have all the same trend and therefore reach to a higher point (i.e. at the lowest vapor qualities). In contrast, for the highest mass flux of 365 $kgm^{-2}s^{-1}$, although the values of performance factor for “CW5” and “CW4” followed the same trend (obtained in the lowest mass flux), for the “CW1” the performance factor reduced with the decrease of vapor quality; the exact opposite of the trend observed for the lowest mass flux. Moreover, a local maximum was observed in PF-x chart at higher vapor qualities for “CW2” and “CW3” suggesting an optimum point at the higher vapor qualities for these two test springs.

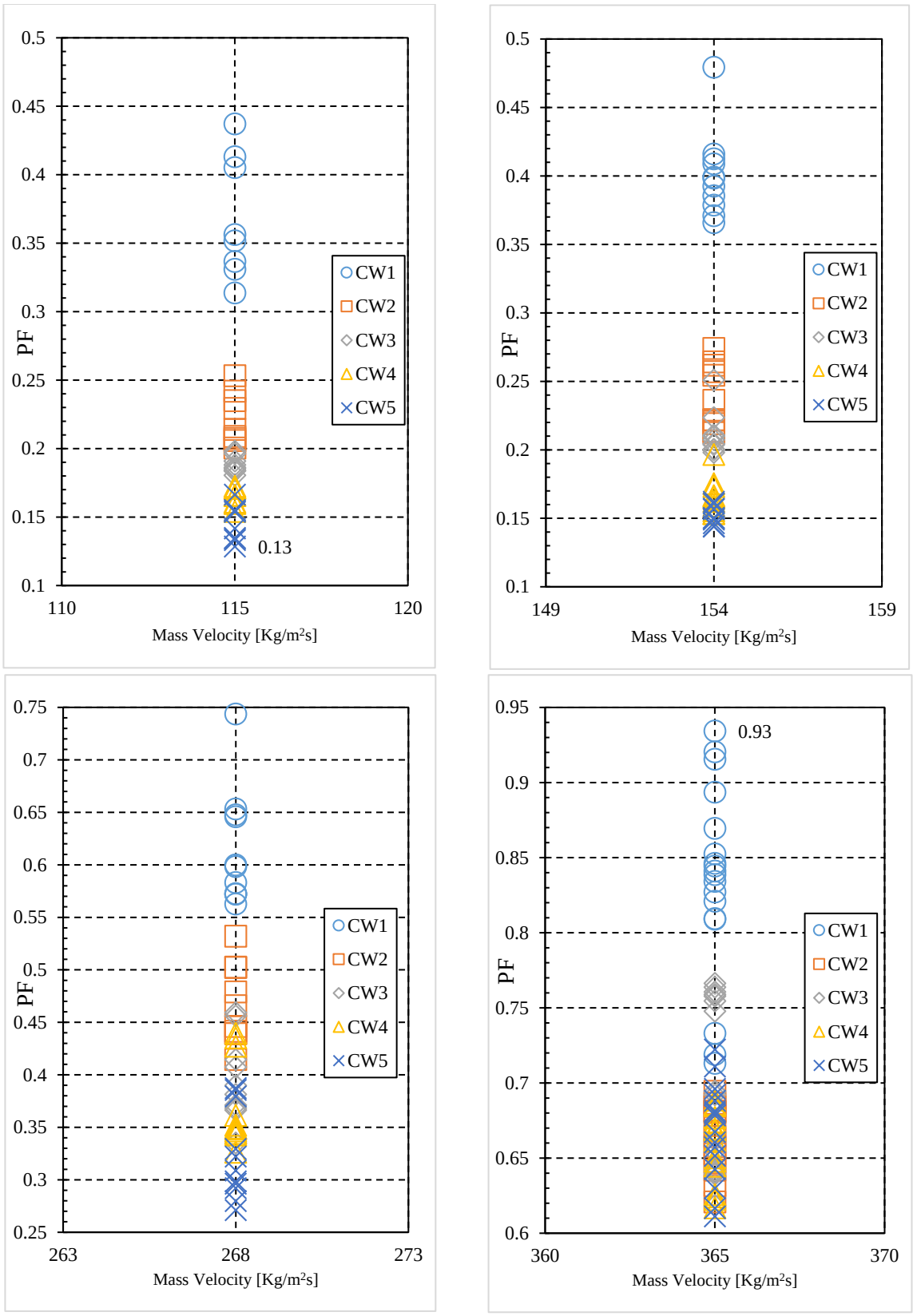

397 **Fig. 10.** The boundary of system performance factor for different inserts under various mass fluxes (kg/m^{2}s).

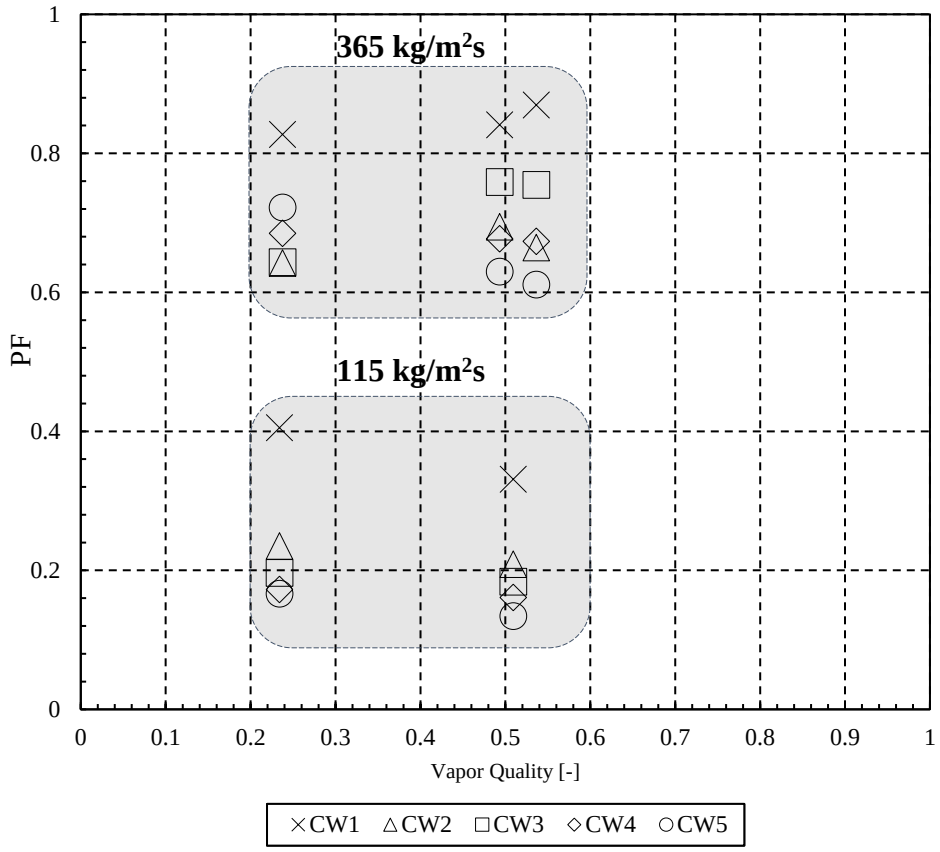

Fig. 11. System performance factor for all inserts under mass velocities of 115 and 365 kg/m^{2}s and different vapor qualities.

4.4. Development of correlation for predicting pressure drops in coiled wire inserted tubes

From the open literature, it is evident that there is no previously developed correlation for predicting the pressure losses of refrigerant R-600a during forced convection condensation in horizontal spiral coil inserted pipes. To develop such a correlation, the proposed correlation by Chisholm, Eq. (5), which was developed for predicting the pressure drops in smooth tubes, is used as the basic formula. Then, in order to consider the influences of spiral coils geometry, different parameters including the coil pitch (P), wire diameter (e), and hydraulic or equivalent diameter (d_e) in the form of coiled wire index (e^2/Pd_e) are implemented, and the following relationship is used:

$$\Delta P_r = \Delta P_s (c_1 + c_2 \frac{e^2}{Pd_e})^{c_3} \quad (21)$$

Where ΔP_r and ΔP_s demonstrate the total pressure drops in the rough pipes and smooth pipe, respectively. Also, d_e is the hydraulic or equivalent diameter.

The combination of geometrical parameters of the coiled wires, i.e. wire diameter (e), coil pitch (P), and tube diameter (d), in the form of coiled wire index was previously introduced and used by Agrawal et al. [9] for taking into account the effects of coiled wire geometry. However, this study uses the coiled wire index in the form of $(\frac{e^2}{Pd_e})$ to take into account the impacts of geometrical parameters. It is worth noting that the tube hydraulic or equivalent diameter is used instead of the tube internal diameter.

To determine the equivalent diameter, the following relation is used:

$$d_e = {}^{4V}\!/_{A} \tag{22}$$

Where V and A represent the total free space volume and the total wet surface, respectively. Finally the equivalent diameter is computed as follows:

$$d_e = {}^{(d^2 - \gamma e)}\!\Big/_{(d + \gamma)} \tag{23}$$

In Eq. (23), γ is calculated by:

$$\gamma = {}^{\pi e(d - e)}\!\Big/_{(Psin\theta)} \tag{24}$$

Where θ is coil helix angle.

Finally, by employing the current experimental data and least square regression analysis, the suggested correlation is achieved:

$$\Delta P_r = \Delta P_s(4.33 + 2702\frac{e^2}{Pd_e})^{0.2956} \tag{25}$$

The predicted pressure drops by the correlation proposed in this study, Eq. (25), are compared to the present experimental results in Fig. 12. As it is observed, most of the predicted values for pressure drops are within an error window of ±30% of the empirical pressure drops results.

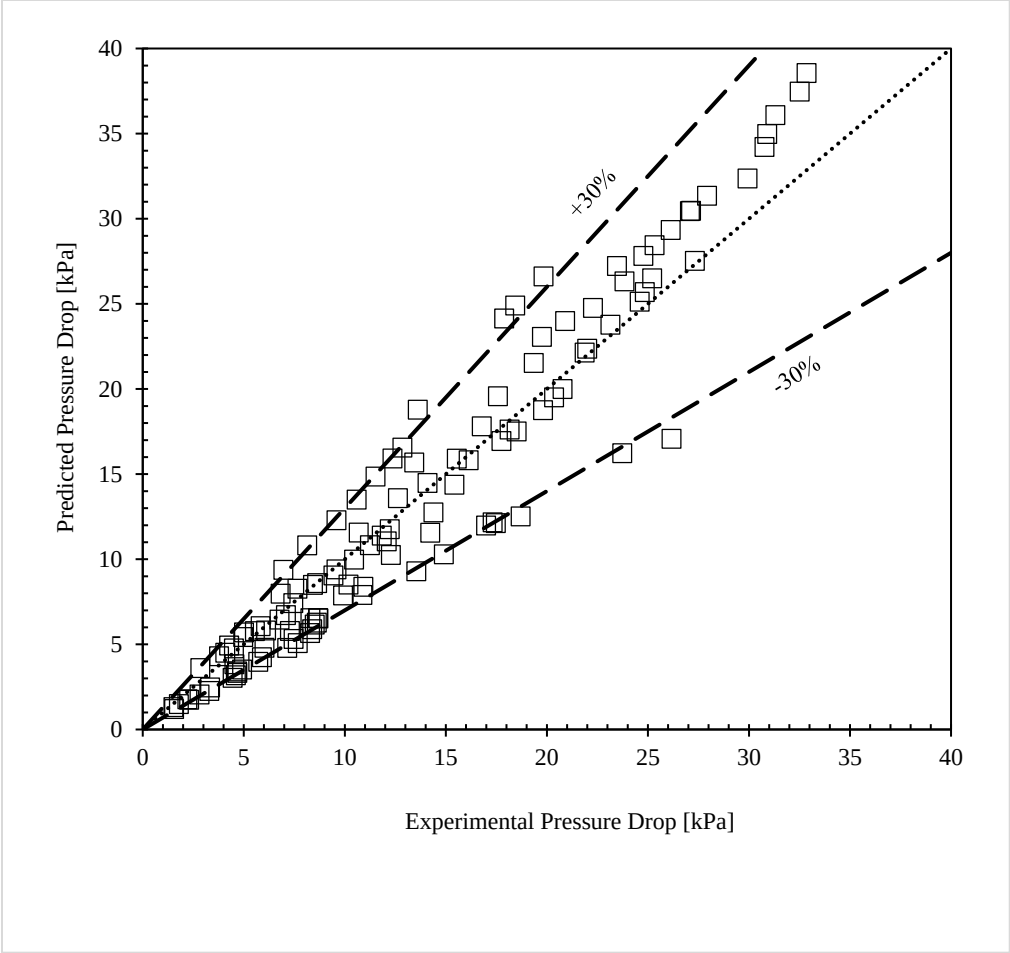

Fig. 12. Comparison between frictional pressure drops obtained by the experiments and the present correlation.

In order to compute the average absolute deviation (AAD) and the average deviation (AD) of the data determined by the new correlation from the experimental results, the following relations are employed:

$$AAD = \frac{1}{N}\left(\sum_{1}^{N}\frac{\left|h_{calculated} - h_{experimental}\right|}{h_{experimental}}\right) \times 100 \tag{26}$$

$$AD = \frac{1}{N}\left(\sum_{1}^{N}\frac{h_{calculated} - h_{experimental}}{h_{experimental}}\right) \times 100 \tag{27}$$

The calculations illustrated that the average deviation and the average absolute deviation of the obtained results by the current correlation from the experimental results are -0.48% and 6.92 %, respectively. The suggested correlation can be used to predict the pressure drops for designing horizontal heat exchangers employing coiled wires.

4.5. Flow pattern

One important phenomenon affecting the thermal performance of heat exchangers in two-phase flows is the flow regime. Generally, the flow regimes observed in a horizontally located pipe are classified as bubble, stratified, stratified-wavy, slug, intermittent, plug, annular and mist flows. In the current research, a sight glass was placed in the cycle to capture the flow patterns. Depending on the operating conditions of the current refrigeration cycle, three different flow patterns including annular, intermittent and stratified-wavy were observed. Fig. 13 illustrates the flow regimes observed during the experiments.

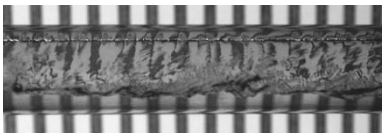

Stratified-wavy (G=154 kg/m^{2}s, x=0.242)

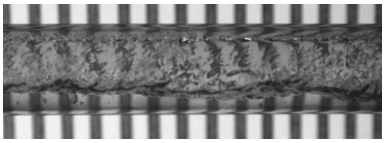

Intermittent (G=154 kg/m^{2}s, x=0.32)

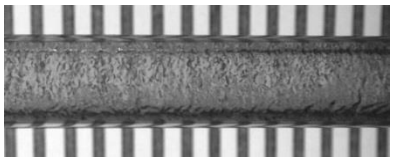

Annular (G=154 kg/m^{2}s, x=0.78)

Fig. 13. Different flow regimes observed during the current experiments.

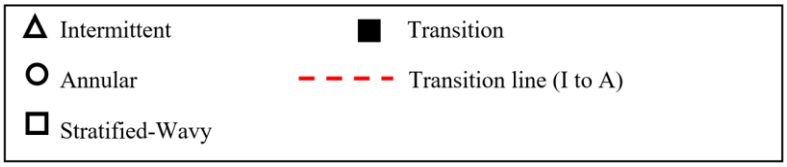

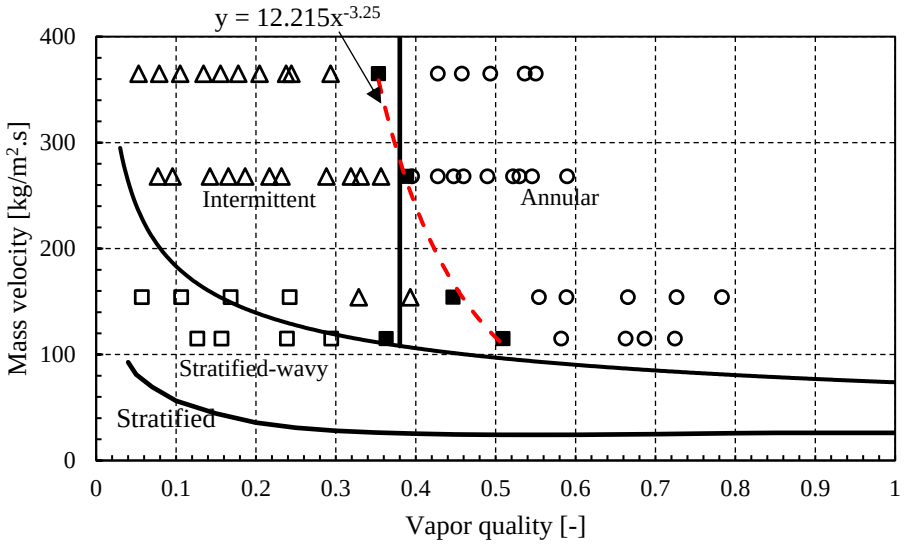

Fig. 14. Comparison between the observed flow patterns for the smooth tube and the El Hajal et al. [46] map.

450

451

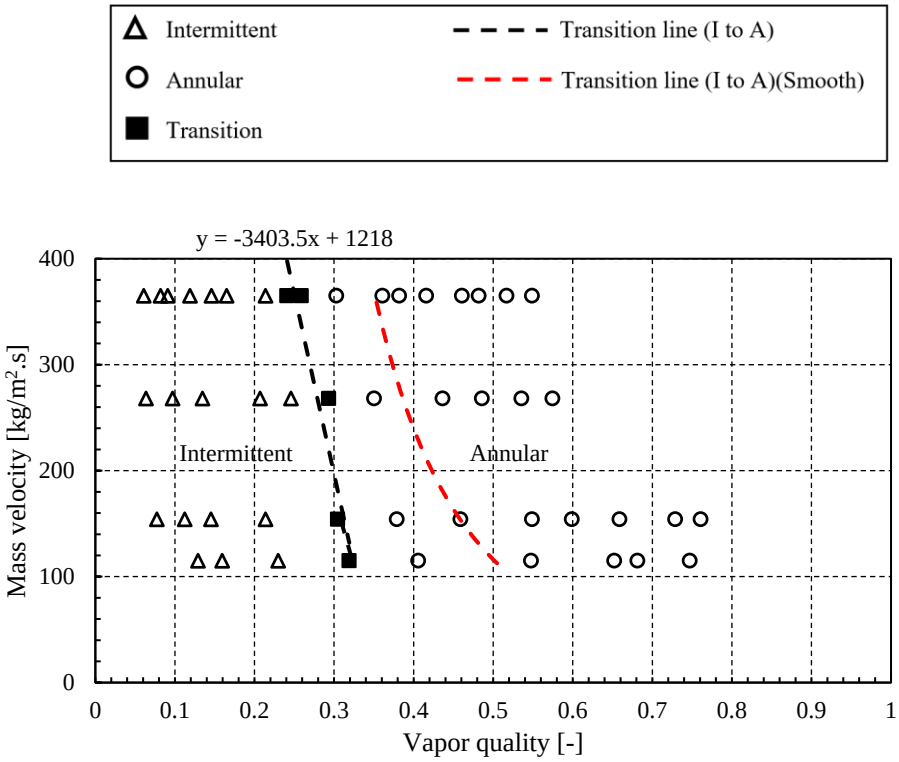

Fig. 15. Observed flow patterns for CW1. Data are reported using the coordinates of the El Hajal et al. [46] map.

452

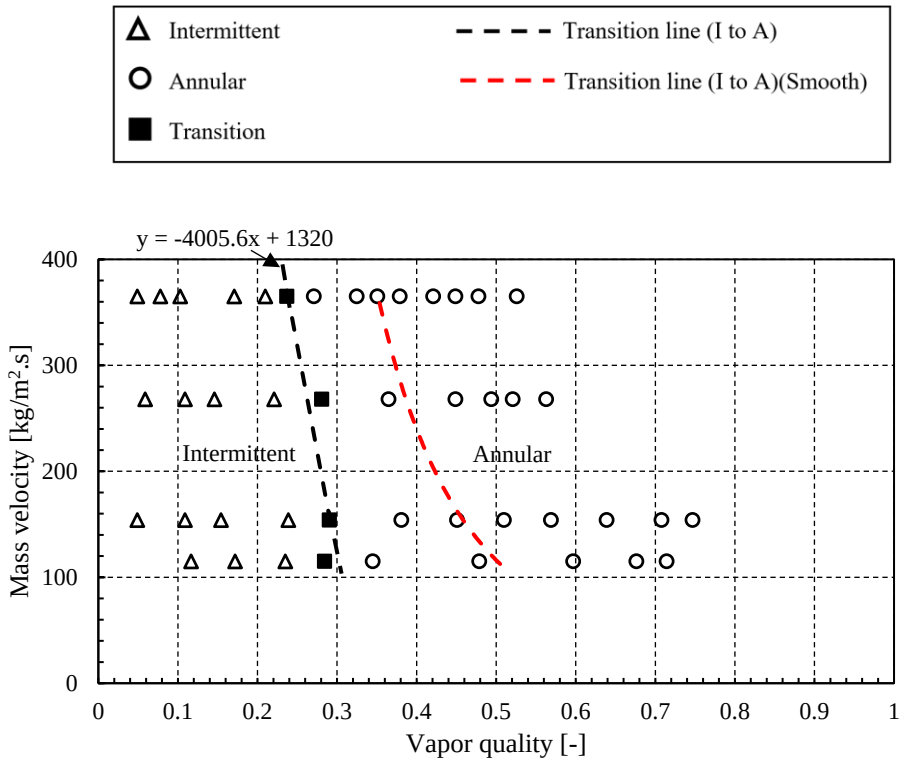

Fig. 16. Observed flow patterns for CW2. Data are reported using the coordinates of the El Hajal et al. [46] map.

453

Intermittent
Annular
Transition
Transition line (I to A)
Transition line (I to A)(Smooth)

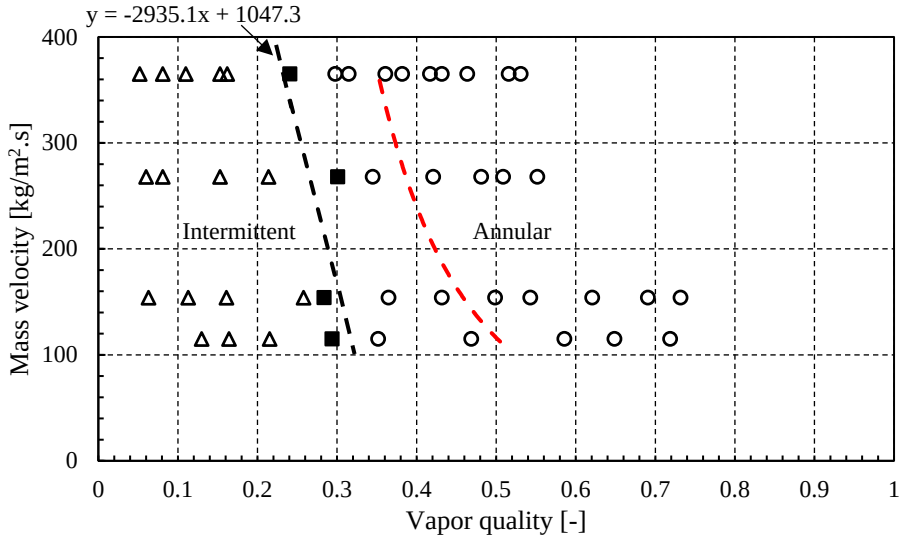

Fig. 11. Observed flow patterns for CW3. Data are reported using the coordinates of the El Hajal et al. [46] map.

454

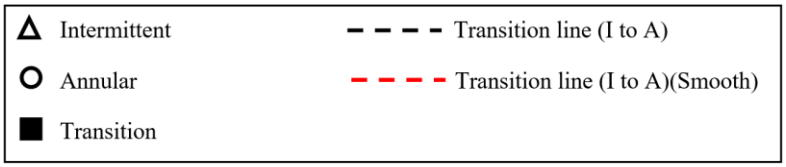

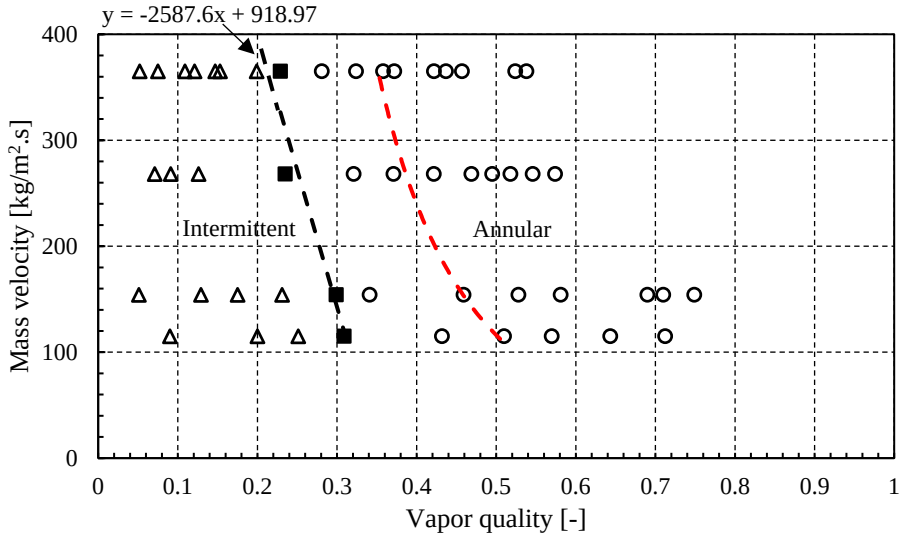

Fig. 18. Observed flow patterns for CW4. Data are reported using the coordinates of the El Hajal et al. [46] map.

455

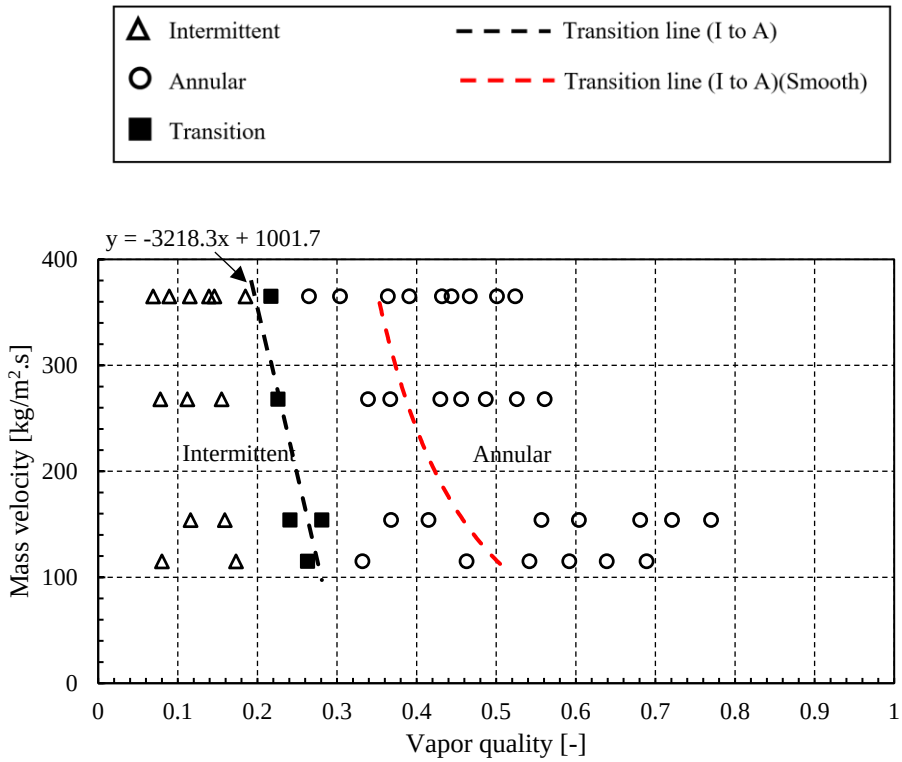

Fig. 19. Observed flow patterns for CW5. Data are reported using the coordinates of the El Hajal et al. [46] map.

Figs. 14-19 depict the flow pattern maps of the refrigerant R-600a for both smooth and coiled wire inserted tubes which are prepared based on the map proposed by El Hajal et al. [46]. As can be seen, the annular flow pattern is observable at higher vapor qualities and mass fluxes. At higher vapor qualities, the volume of liquid refrigerant is less. Therefore, the shear stress between the two phases could dominate the gravity force. As a consequence, the liquid refrigerant expands on the inner surface of the tube and the vapor refrigerant flows in the tube core resulting in the annular flow regime.

On the contrary, at lower vapor qualities the volume of the liquid refrigerant is higher. Hence, the gravity force dominates the shear stress between the two phases. Under these conditions, the liquid refrigerant flows at the bottom of the pipe. Therefore, stratified-wavy or intermittent flow regimes are observable depending on the mass velocity.

It is also noticeable from the smooth tube map, Fig. 14, that there is a good consistency between the transition lines observed during the experiments and those presented by the map of El Hajal et al. [46]. Among these flow regimes, the annular flow regime is found to be attractive due to the higher rates of heat transfer obtained through this mechanism. The annular flow pattern consists of a layer of liquid refrigerant distributed on the tube inner surface and the vapor phase flowing in the tube core [47]. The maps illustrate that inserting the coiled wires postpones the transition of flow regimes from annular to intermittent. For the case of the smooth tube, the transition from annular to intermittent takes place at the vapor quality of about 0.4, while that

transition for the coiled wire inserted tubes take place at the vapor quality of about 0.3. For the smooth tube the earliest transition from the annular to intermittent regime occurred at mass flux of 115 $kgm^{-2}s^{-1}$ and vapor quality of 0.51, while the latest transition occurred at mass flux of 365 $kgm^{-2}s^{-1}$ and vapor quality of 0.35. For the spiral coil inserted tubes the earliest transition happened for CW1 (G=115 $kgm^{-2}s^{-1}$, x=0.32) and the latest transition took place for CW5 (at G=365 $kgm^{-2}s^{-1}$, x=0.21) which has the highest pressure drop and highest heat transfer coefficient [23]. Insertion of the spiral coils establishes a swirling flow which contributes to the distribution of the liquid refrigerant on the inner surface of tube circumference which in turn helps the existence of annular flow at lower vapor qualities.

5. Conclusion

An empirical study is conducted to appraise the pressure drop growth of refrigerant R-600a during condensation in horizontal plain and spiral coil inserted pipes, where the vapor quality and the refrigerant mass velocity varied between 0.05-0.79 and 115-365 $kgm^{-2}s^{-1}$, respectively. As employing the inserts resulted in increase of both heat transfer and pressure drop data, the system performance factor is calculated to illuminate the effectiveness of these devices. Furthermore, a new correlation is proposed to predict the pressure drops of R-600a in horizontal spiral coil inserted tubes. Finally, new flow pattern maps are presented for the coiled wire inserted pipes. The main conclusions are as follows:

- The pressure loss augmented by the increment of the vapor quality and refrigerant mass velocity for both plain and coiled wire inserted tubes.
- Installing coiled wires inside the horizontal tubes resulted in augmentation of the pressure losses. However, the value of the pressure loss increment is a function of the operational conditions and the inserts geometry.
- The values of the pressure drops increased by increasing the wire diameter and decreasing the coil pitch.
- The system performance factor was below one for all mass fluxes and vapor qualities. However, the higher performance factors were obtained for higher mass velocities, because the pressure drop growth above the smooth tube in higher mass fluxes is not significant as it is in lower mass fluxes.
- Based on the present empirical data, a new correlation with an accuracy of ±30% is suggested for predicting the pressure loss of R-600a during condensation inside horizontal spring inserted pipes.
- Three flow regimes including stratified-wavy, intermittent, and annular were observed. The flow pattern maps showed that installing coiled wires postponed the transition of flow regimes from annular to intermittent.

6. Appendix

6.1. Calculation of uncertainties for mass flux

To compute the uncertainty of the mass flux, the Eq. (A-1) proposed by Schultz and Cole [28] is used. By substituting the mass flux relation, Eq. (A-2) in the Eq. (A-1), Eq. (A-3) is obtained as follows:

$$U_R = \left[\sum_{i=1}^{n}\left(\frac{\partial R}{\partial V_i}U_{V_i}\right)^2\right]^{\frac{1}{2}} \tag{A-1}$$

$$G = \frac{\dot{m}}{\pi\frac{d^2}{4}} \tag{A-2}$$

$$U_G = \left[\left(\frac{U_{\dot{m}}}{\pi\frac{d^2}{4}}\right)^2 + \left(-8\frac{\dot{m}}{\pi d^3}U_d\right)^2\right]^{1/2} \tag{A-3}$$

Therefore, the uncertainties for different mass fluxes are calculated as follows:

$$U_{G=365} = \left[\left(\frac{0.001}{\pi\frac{0.0081^2}{4}}\right)^2 + \left(-8\frac{0.019}{\pi\times 0.0081^3}\times 0.0005\right)^2\right]^{1/2} = 24.4$$

$$\%U_G = \left(\frac{U_G}{G}\right)\times 100 = \frac{24.4}{365}\times 100 = 6.68\%$$

$$U_{G=268} = \left[\left(\frac{0.001}{\pi\frac{0.0081^2}{4}}\right)^2 + \left(-8\frac{0.014}{\pi\times 0.0081^3}\times 0.0005\right)^2\right]^{1/2} = 22.14$$

$$\%U_G = \left(\frac{U_G}{G}\right)\times 100 = \frac{22.14}{268}\times 100 = 8.26\%$$

$$U_{G=154} = \left[\left(\frac{0.001}{\pi\frac{0.0081^2}{4}}\right)^2 + \left(-8\frac{0.0083}{\pi\times 0.0081^3}\times 0.0005\right)^2\right]^{1/2} = 20.41$$

$$\%U_G = \left(\frac{U_G}{G}\right)\times 100 = \frac{20.41}{154}\times 100 = 13.25\%$$

$$U_{G=115} = \left[\left(\frac{0.001}{\pi\frac{0.0081^2}{4}}\right)^2 + \left(-8\frac{0.0061}{\pi\times 0.0081^3}\times 0.0005\right)^2\right]^{1/2} = 19.95$$

$$\%U_G = \left(\frac{U_G}{G}\right)\times 100 = \frac{19.95}{115}\times 100 = 17.35\%$$

6.2. Calculation of uncertainties for frictional pressure drop

Considering Eq. (2), the frictional pressure drop is determined as follows:

$$\Delta P_{tot} = \Delta P_{mom} + \Delta P_{fric} \tag{A-4}$$

Therefore, based on Eq. (A-1):

$$U_{\Delta P_{fric}} = \left[\left(U_{\Delta P_{tot}}\right)^2 + \left(U_{\Delta P_{mom}}\right)^2\right]^{1/2} \tag{A-5}$$

Considering the information provided in Table 3:

$$U_{\Delta P_{tot}} = 0.00075$$

By taking into account the Eq. (3):

$$U_{\Delta P_{mom}} = \left[\left(\frac{\partial \Delta P_{mom}}{\partial G} U_G\right)^2 + \left(\frac{\partial \Delta P_{mom}}{\partial x} U_x\right)^2 + \left(\frac{\partial \Delta P_{mom}}{\partial \varepsilon} U_\varepsilon\right)^2\right]^{\frac{1}{2}}$$

Therefore, after derivation we have:

$$\begin{aligned} U_{\Delta P_{mom}} = \Bigg[& \left(2GU_G\left\{\left[\frac{(1-x)^2}{\rho_l(1-\varepsilon)} + \frac{x^2}{\rho_g \varepsilon}\right]_{out} - \left[\frac{(1-x)^2}{\rho_l(1-\varepsilon)} + \frac{x^2}{\rho_g \varepsilon}\right]_{in}\right\}\right)^2 \\ & + \left(G_{tot}^2\left\{\left[\frac{-2xU_x}{\rho_l(1-\varepsilon)} + \frac{2xU_x}{\rho_g \varepsilon}\right]_{out} - \left[\frac{-2xU_x}{\rho_l(1-\varepsilon)} + \frac{2xU_x}{\rho_g \varepsilon}\right]_{in}\right\}\right)^2 \\ & + \left(G_{tot}^2\left\{\left[\frac{(1-x)^2 U_\varepsilon}{\rho_l(1-\varepsilon)^2} + \frac{-x^2 U_\varepsilon}{\rho_g \varepsilon^2}\right]_{out} - \left[\frac{(1-x)^2 U_\varepsilon}{\rho_l(1-\varepsilon)^2} + \frac{-x^2 U_\varepsilon}{\rho_g \varepsilon^2}\right]_{in}\right\}\right)^2\Bigg]^{1/2} \end{aligned}$$

Where $U_G = 17.35\%$ and $U_x = 6\%$. Considering the uncertainty of vapor quality from the previous study [23]:

$$\begin{aligned} U_x = \Bigg\{ & \left[\frac{\gamma_e I U_V}{\dot{m}_{ref} h_{fg,e}}\right]^2 + \left[\frac{\gamma_e V U_I}{\dot{m}_{ref} h_{fg,e}}\right]^2 + \left[\frac{\gamma_e V I U_{\dot{m}_{ref}}}{\dot{m}_{ref}{}^2 h_{fg,e}}\right]^2 + 2\left[\frac{C_p U_T}{h_{fg,e}}\right]^2 \\ & + \left[\frac{\gamma_c C_{p,w}\left(T_{w,out} - T_{w,in}\right) U_{\dot{m}_w}}{\dot{m}_{ref} h_{fg,e}}\right]^2 + 2\left[\frac{\gamma_c C_{p,w} \dot{m}_w U_{T_w}}{\dot{m}_{ref} h_{fg,e}}\right]^2\Bigg\}^{1/2} \end{aligned}$$

Based on the correlation of Zivi [48] and after derivation:

$$U_\varepsilon = \frac{U_x(\frac{\rho_g}{\rho_l})^{2/3}}{\left[1+\left(\frac{1-x_{tc}}{x_{tc}}\right)\left(\frac{\rho_g}{\rho_l}\right)^{\frac{2}{3}}\right]^2 {x_{tc}}^2}$$

In order to explain the effect of predicted void fraction accuracy on uncertainty of momentum equation (and therefore its frictional one); the highest momentum pressure drop which is related to the highest mass flow rate and the relevant frictional pressure drop during experiments (related to CW5) are prepared in the following table.

Table A-1. The operating conditions associated with the highest pressure drops.

Vapor quality	Mass flow rate ($kgm^{-2}s^{-1}$)	void fraction	Momentum Pressure Drop (kPa)	Frictional Pressure Drop (kPa)
0.524	365	0.9289	2.2575	40.54

Based on the values presented in Table A-1:

$U_\varepsilon = 1.6\%$

Therefore:

$$U_{\Delta P_{fric}} = \left[\left(U_{\Delta P_{tot}}\right)^2 + \left(U_{\Delta P_{mom}}\right)^2\right]^{1/2} = [(0.00075)^2 + (0.07)^2]^{1/2} = 7\%$$

6.3. Evaluation of repeatability of the tests

To verify the correct performance of the cycle and the accuracy of experimental data, 25% of the test runs for the case of smooth tube were repeated at different times. Table A-2 presents the values of the vapor qualities and frictional pressure drops obtained during the first and second test runs under different mass velocities. The average deviation and average absolute deviation of the obtained values for the vapor quality are 0.93 and 3.55%, respectively. Furthermore, these deviations for the frictional pressure drop are 1.08 and 3.02%, respectively. The results show that the deviations of the obtained vapor qualities and frictional pressure drops during the second test runs with respect to the primary data are appropriate the tests are repeatable.

Table A-2. Results of the repeatability tests for the case of smooth tube.

First run			Second run		Deviation of second run from first run (%)	
Mass velocity ($kgm^{-2}s^{-1}$)	Vapor quality (-)	Frictional pressure drop (kPa)	Vapor quality (-)	Frictional pressure drop (kPa)	Vapor quality	Frictional pressure drop

115	0.12079	0.60242	0.1291	0.65352	6.88	8.48
115	0.3654	1.0384	0.3766	1.1096	3.07	6.86
115	0.5877	1.4602	0.577	1.4267	-1.82	-2.29
154	0.2424	1.523	0.2523	1.6042	4.08	5.33
154	0.4467	2.322	0.431	2.2218	-3.51	-4.32
154	0.7265	2.874	0.7347	2.9066	1.13	1.13
268	0.1654	2.488	0.1547	2.4079	-6.47	-3.22
268	0.3888	4.424	0.3787	4.3396	-2.59	-1.91
268	0.4899	4.955	0.4992	5.0065	1.89	1.04
268	0.5897	5.483	0.5786	5.384	-1.88	-1.81
365	0.07888	3.652	0.08578	3.7277	8.75	2.07
365	0.2046	6.798	0.2097	6.9029	2.49	1.54
365	0.3534	9.6146	0.3641	9.7558	3.03	1.47
365	0.5365	11.83	0.5253	11.7341	-2.09	0.81

7. Conflict of Interests:

'Declarations of interest: none'

8. References

[1] B. Kumar, G. P. Srivastava, M. Kumar, and A. K. Patil, "A review of heat transfer and fluid flow mechanism in heat exchanger tube with inserts," *Chemical Engineering and Processing-Process Intensification,* vol. 123, pp. 126-137, 2018.

[2] M. Sheikholeslami, M. Gorji-Bandpy, and D. D. Ganji, "Review of heat transfer enhancement methods: Focus on passive methods using swirl flow devices," *Renewable and Sustainable Energy Reviews,* vol. 49, pp. 444-469, 2015.

[3] H. Moradi, A. Bagheri, M. Shafaee, and S. Khorasani, "Experimental investigation on the thermal and entropic behavior of a vertical helical tube with none-boiling upward air-water two-phase flow," *Applied Thermal Engineering,* vol. 157, p. 113621, 2019.

[4] Y. Hong, J. Du, S. Wang, S.-M. Huang, and W.-B. Ye, "Heat transfer and fluid flow behaviors in a tube with modified wire coils," *International Journal of Heat and Mass Transfer,* vol. 124, pp. 1347-1360, 2018.

[5] M. Omara and M. A. Abdelatief, "Experimental study of heat transfer and friction factor inside elliptic tube fixed with helical coils," *Applied Thermal Engineering,* vol. 134, pp. 407-418, 2018.

[6] E. Gholamalizadeh, E. Hosseini, M. B. Jamnani, A. Amiri, and A. Alimoradi, "Study of intensification of the heat transfer in helically coiled tube heat exchangers via coiled wire inserts," *International Journal of Thermal Sciences,* vol. 141, pp. 72-83, 2019.

[7] R. Yun, J.-S. Hwang, J. T. Chung, and Y. Kim, "Flow boiling heat transfer characteristics of nitrogen in plain and wire coil inserted tubes," *International Journal of Heat and Mass Transfer,* vol. 50, pp. 2339-2345, 2007.

[8] M. Shafaee, F. Alimardani, and S. Mohseni, "An empirical study on evaporation heat transfer characteristics and flow pattern visualization in tubes with coiled wire inserts," *International Communications in Heat and Mass Transfer,* vol. 76, pp. 301-307, 2016.

[9] K. Agrawal, A. Kumar, M. A. Behabadi, and H. Varma, "Heat transfer augmentation by coiled wire inserts during forced convection condensation of R-22 inside horizontal tubes," *International journal of multiphase flow,* vol. 24, pp. 635-650, 1998.

[10] M. Akhavan-Behabadi, M. Salimpour, and V. Pazouki, "Pressure drop increase of forced convective condensation inside horizontal coiled wire inserted tubes," *International Communications in Heat and Mass Transfer,* vol. 35, pp. 1220-1226, 2008.
[11] M. Akhavan-Behabadi, S. Mohseni, H. Najafi, and H. Ramazanzadeh, "Heat transfer and pressure drop characteristics of forced convective evaporation in horizontal tubes with coiled wire inserts," *International Communications in Heat and Mass Transfer,* vol. 36, pp. 1089-1095, 2009.
[12] E. Jalil and K. Goudarzi, "Experimental study of heat transfer enhancement in the evaporator of single-effect absorption chiller using new different tube insert," *Applied Thermal Engineering,* vol. 128, pp. 1-9, 2018.
[13] M. Sharafeldeen, N. Berbish, M. Moawed, and R. Ali, "Experimental investigation of heat transfer and pressure drop of turbulent flow inside tube with inserted helical coils," *Heat and Mass Transfer,* vol. 53, pp. 1265-1276, 2017.
[14] J. Du, Y. Hong, S. Wang, W.-B. Ye, and S.-M. Huang, "Experimental thermal and flow characteristics in a traverse corrugated tube fitted with regularly spaced modified wire coils," *International Journal of Thermal Sciences,* 2018.
[15] K. A. Hamid, W. Azmi, R. Mamat, and K. Sharma, "Heat transfer performance of TiO2–SiO2 nanofluids in a tube with wire coil inserts," *Applied Thermal Engineering,* vol. 152, pp. 275-286, 2019.
[16] Z. Yang, M. Gong, G. Chen, X. Zou, and J. Shen, "Two-phase flow patterns, heat transfer and pressure drop characteristics of R600a during flow boiling inside a horizontal tube," *Applied Thermal Engineering,* vol. 120, pp. 654-671, 2017.
[17] H. A. Moghaddam, M. Shafaee, and R. Riazi, "Numerical Investigation of a Refrigeration Ejector: Effects of Environment-Friendly Refrigerants and Geometry of the Ejector Mixing Chamber," *European Journal of Sustainable Development Research,* vol. 3, p. em0090, 2019.
[18] M. Rasti, M. Hatamipour, S. Aghamiri, and M. Tavakoli, "Enhancement of domestic refrigerator's energy efficiency index using a hydrocarbon mixture refrigerant," *Measurement,* vol. 45, pp. 1807-1813, 2012.
[19] J. Copetti, M. Macagnan, and F. Zinani, "Experimental study on R-600a boiling in 2.6 mm tube," *international journal of refrigeration,* vol. 36, pp. 325-334, 2013.
[20] M.-Y. Wen, K.-J. Jang, and C.-Y. Ho, "The characteristics of boiling heat transfer and pressure drop of R-600a in a circular tube with porous inserts," *Applied thermal engineering,* vol. 64, pp. 348-357, 2014.
[21] J. D. de Oliveira, J. B. Copetti, and J. C. Passos, "Experimental investigation on flow boiling pressure drop of R-290 and R-600a in a horizontal small tube," *International Journal of Refrigeration,* vol. 84, pp. 165-180, 2017.
[22] Z.-Q. Yang, G.-F. Chen, Y. Yao, Q.-L. Song, J. Shen, and M.-Q. Gong, "Experimental study on flow boiling heat transfer and pressure drop in a horizontal tube for R1234ze (E) versus R600a," *International Journal of Refrigeration,* vol. 85, pp. 334-352, 2018.
[23] H. A. Moghaddam, A. Sarmadian, and M. Shafaee, "An experimental study on condensation heat transfer characteristics of R-600a in tubes with coiled wire inserts," *Applied Thermal Engineering,* p. 113889, 2019.
[24] B. Ghorbani, M. Akhavan-Behabadi, S. Ebrahimi, and K. Vijayaraghavan, "Experimental investigation of condensation heat transfer of R600a/POE/CuO nano-refrigerant in flattened tubes," *International Communications in Heat and Mass Transfer,* vol. 88, pp. 236-244, 2017.
[25] Z.-Q. Yang, G.-F. Chen, Y.-X. Zhao, Q.-X. Tang, H.-W. Xue, Q.-L. Song*, et al.*, "Experimental study on flow boiling heat transfer of a new azeotropic mixture of R1234ze (E)/R600a in a horizontal tube," *International Journal of Refrigeration,* vol. 93, pp. 224-235, 2018.
[26] J. G. Collier and J. R. Thome, *Convective boiling and condensation*: Clarendon Press, 1994.

[27] S. Zivi, "Estimation of steady-state steam void-fraction by means of the principle of minimum entropy production," *Journal of heat transfer,* vol. 86, pp. 247-251, 1964.
[28] R. Schultz and R. Cole, "Uncertainty analysis in boiling nucleation," in *AIChE symposium series*, 1979, pp. 32-38.
[29] V. Hejazi, M. Akhavan-Behabadi, and A. Afshari, "Experimental investigation of twisted tape inserts performance on condensation heat transfer enhancement and pressure drop," *International Communications in Heat and Mass Transfer,* vol. 37, pp. 1376-1387, 2010.
[30] F. Alimardani, H. A. Moghaddam, A. Sarmadian, and M. Shafaee, "Pressure loss and performance assessment of horizontal spiral coil inserted pipes during forced convective evaporation of R-600a," *International Journal of Refrigeration,* 2019.
[31] D. Chisholm, "Pressure gradients due to friction during the flow of evaporating two-phase mixtures in smooth tubes and channels," *International Journal of Heat and Mass Transfer,* vol. 16, pp. 347-358, 1973.
[32] H. Müller-Steinhagen and K. Heck, "A simple friction pressure drop correlation for two-phase flow in pipes," *Chemical Engineering and Processing: Process Intensification,* vol. 20, pp. 297-308, 1986.
[33] L. Friedel, "Improved friction pressure drop correlation for horizontal and vertical two-phase pipe flow," *Proc. of European Two-Phase Flow Group Meet., Ispra, Italy, 1979,* 1979.
[34] M. Macdonald and S. Garimella, "Hydrocarbon condensation in horizontal smooth tubes: Part I–Measurements," *International Journal of Heat and Mass Transfer,* vol. 93, pp. 75-85, 2016.
[35] C. L. Ong and J. R. Thome, "Experimental Adiabatic Two-Phase Pressure Drops of R134a, R236fa and R245fa in Small Horizontal Circular Channels," in *ASME/JSME 2011 8th Thermal Engineering Joint Conference*, 2011.
[36] A. Dalkilic, "Condensation pressure drop characteristics of various refrigerants in a horizontal smooth tube," *International Communications in Heat and Mass Transfer,* vol. 38, pp. 504-512, 2011.
[37] Q. Song, G. Chen, H. Guo, J. Shen, and M. Gong, "Two-phase flow condensation pressure drop of R14 in a horizontal tube: Experimental investigation and correlation development," *International Journal of Heat and Mass Transfer,* vol. 139, pp. 330-342, 2019.
[38] Y. Gao, S. Shao, B. Zhan, Y. Chen, and C. Tian, "Heat transfer and pressure drop characteristics of ammonia during flow boiling inside a horizontal small diameter tube," *International Journal of Heat and Mass Transfer,* vol. 127, pp. 981-996, 2018.
[39] X. Zhuang, G. Chen, X. Zou, Q. Song, and M. Gong, "Experimental investigation on flow condensation of methane in a horizontal smooth tube," *International Journal of Refrigeration,* vol. 78, pp. 193-214, 2017.
[40] R. Andrzejczyk, T. Muszynski, and C. A. Dorao, "Experimental investigations on adiabatic frictional pressure drops of R134a during flow in 5 mm diameter channel," *Experimental Thermal and Fluid Science,* vol. 83, pp. 78-87, 2017.
[41] M. M. Mahmoud, T. G. Karayiannis, and D. B. Kenning, "Flow Boiling Pressure Drop of R134a in Microdiameter Tubes: Experimental Results and Assessment of Correlations," *Heat Transfer Engineering,* vol. 35, pp. 178-192, 2014.
[42] M. R. Salimpour and H. Gholami, "Effect of inserting coiled wires on pressure drop of R-404A condensation," *International Journal of Refrigeration,* vol. 40, pp. 24-30, 2014.
[43] K. Agrawal and H. Varma, "Experimental study of heat transfer augmentation versus pumping power in a horizontal R12 evaporator," *International journal of refrigeration,* vol. 14, pp. 273-281, 1991.
[44] M. Shafaee, H. Mashouf, A. Sarmadian, and S. Mohseni, "Evaporation heat transfer and pressure drop characteristics of R-600a in horizontal smooth and helically dimpled tubes," *Applied Thermal Engineering,* vol. 107, pp. 28-36, 2016.

[45] A. Sarmadian, M. Shafaee, H. Mashouf, and S. Mohseni, "Condensation heat transfer and pressure drop characteristics of R-600a in horizontal smooth and helically dimpled tubes," *Experimental Thermal and Fluid Science,* vol. 86, pp. 54-62, 2017.

[46] J. El Hajal, J. R. Thome, and A. Cavallini, "Condensation in horizontal tubes, part 1: two-phase flow pattern map," *International Journal of Heat and Mass Transfer,* vol. 46, pp. 3349-3363, 2003.

[47] H. Mashouf, M. Shafaee, A. Sarmadian, and S. Mohseni, "Visual study of flow patterns during evaporation and condensation of R-600a inside horizontal smooth and helically dimpled tubes," *Applied Thermal Engineering,* vol. 124, pp. 1392-1400, 2017.

[48] S. Zivi, "Estimation of steady-state steam void-fraction by means of the principle of minimum entropy production," 1964.